ULTRA WIDEBAND SYNTHETIC APERTURE IMAGE FORMATION TECHNIQUES

H.A. Khan*, W.Q. Malik*, D.J. Edwards*, C.J. Stevens*

*Department of Engineering Science, University of Oxford, Parks Road, Oxford OX1 3PJ, UK
Email: {hammad.khan, wasim.malik, david.edwards, christopher.stevens}@eng.ox.ac.uk

KEYWORDS: Ultra wideband (UWB), synthetic aperture radar, radio imaging, angle of arrival (AoA), vector network analyser (VNA).

ABSTRACT

This paper presents the experimental results of a UWB based imaging system. Radio imaging of a room is performed using an imaging technique based upon the angle-of-arrival (AoA) information through the use of a synthetic aperture. These images are actually a visual representation of the multipaths and have the ability to distinguish between temporally stationary and varying components. The paper describes the measurement and signal processing techniques used to acquire the imaging information. This groundwork can be used for UWB indoor radio channel characterisation and also for optimal design of UWB systems that can be used in applications ranging from multipath-resistant communications systems to ground-penetrating radar (GPR) and medical imaging.

1 INTRODUCTION

Radio imaging is a well-known technique used for landmine detection, wall imaging, search-and-rescue operations, motion tracking, propagation environment characterisation, and surveillance [1, 2]. Microwave Doppler radar has been in use for some of these applications for more than a decade, but it suffers from range limitations and false alarm triggering [3, 4]. Research has been underway for designing suitable ultra wideband (UWB) systems that can be used for radar-type imaging applications [5-9]. The key benefits of this technique are material characterisation capability, high time-resolution, ability to distinguish between foliage and human activity, low probability of interception, and innocuous electromagnetic operation [8]. In this paper, we present the results of a UWB radio imaging study based on measurements conducted in a controlled indoor wireless propagation environment. We extract the angle-of-arrival (AoA) information through a synthetic aperture [10] with UWB waveforms using a vector network analyser (VNA) based technique [11]. This information is then processed to obtain two dimensional power spectrum plots on azimuth-elevation axes, giving a visual representation of multipath arrivals.

2 IMAGING SCENARIO

We performed the UWB imaging measurements using an indoor channel. The environment consisted of a medium-sized room with computers, wooden desks, and some metallic cabinets. The transmitting and receiving antennas were at a height of 1.5 m from the ground and separated by 3.7 m. A computer-controlled vector network analyser (VNA) [11] was used to sound the channel with 20dBm power at 4-6 GHz. This corresponds to 40% fractional bandwidth. The complex channel transfer function was measured at 401 discrete frequency points (i.e. a resolution of 5MHz). The receiving antenna moved over a synthetic aperture of 10 cm x 10 cm area by taking 100 measurements using a spatial resolution of 1 cm. An unobstructed line of sight was present between the antennas throughout the measurements. This is shown in Fig. 1.

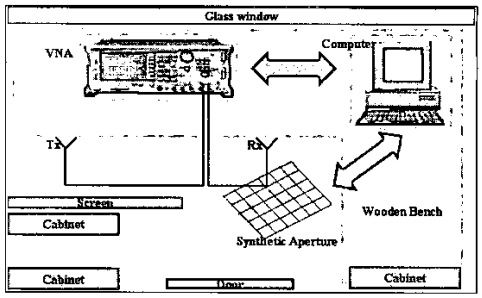

Figure 1. Experimental environment for the imaging scenario.

The channel is considered to be constant and hence we can assume that all the data is measured at the same time, which makes the signal processing easier.

3 IMAGING ALGORITHM

There have been several imaging and AoA algorithms developed over the years [10]. But most of these algorithms assume a narrowband condition and only a few are suited for a wide angle multipath environment with correlated signals [12]. In the narrowband case, the time resolution for processing the received signals is very poor

(because the time resolution is the inverse of the bandwidth), and hence no direct time delay information is available. Traditionally, the improvement in the angle measurement is achieved by increasing the physical aperture size of the receiving antenna. We can alternatively use a synthetic aperture and sample the received signal at a smaller number of points and then apply some signal processing techniques to achieve the same angle resolution. This technique is already established with narrowband systems [10, 12]. Narrowband systems have a number of well-established methods for AoA calculations. These are based on the computation of the power spectral peaks and finding the best estimator for the angle through a variety of estimation methods [10]. We use an imaging algorithm based on the work of Moss et. al. [12] and apply it to UWB. We calculate a power spectrum for the azimuth and elevation angles and plot them on elevation-azimuth axes to present a visual image of how much power is coming from a given set of azimuth and elevation. Since we are using a single plane measurement, we have an up down ambiguity (which can be resolved by taking measurements in two planes) [2]. The complex channel transfer function data is smoothed by using a window function in the spatial domain as well as in the frequency domain.

Let us define some variables based on Moss et. al. [12]. $H(x,y,f)$ is the complex channel transfer function as measured by the VNA at a point (x,y) and at the frequency f, after applying suitable frequency and spatial windows. X and Y are the total numbers of grid positions in each of the horizontal directions of the synthetic aperture (10 each in our experiment). F is the total number of discrete frequency points used (401 in our experiment). $\vec{k}$ is the wave-vector of the propagating electromagnetic wave with the wavenumber being equal to $2\pi/\lambda$ for each wavelength λ. θ and ϕ are the elevation and azimuth, respectively, of the received signal direction relative to the receiver. The components of the wave-vector are

$$\begin{aligned} k_x &= (2\pi/\lambda)\cos\phi\cos\theta \\ k_y &= -(2\pi/\lambda)\sin\phi\cos\theta \\ k_z &= (2\pi/\lambda)\sin\theta \end{aligned} \qquad (1)$$

If $\vec{R}$ is the position vector from the transmitter to the receiving point, then the power spectrum at a particular time incident is given by equation (2),

$$P(t,\theta,\phi) = \left| \sum_{f=1}^{F} \sum_{x=1}^{X} \sum_{y=1}^{Y} H(x,y,f) e^{-i(\vec{k}.\vec{R})} e^{-i\omega t} \right|^2 \qquad (2)$$

or we can just use the amplitude spectrum as given by equation (3)

$$A(t,\theta,\phi) = \left| \sum_{f=1}^{F} \sum_{x=1}^{X} \sum_{y=1}^{Y} H(x,y,f) e^{-i(\vec{k}.\vec{R})} e^{-i\omega t} \right| \qquad (3)$$

The frequency and spatial windowing has already been applied on the complex channel transfer function to achieve sidelobe suppression. The presence of three summation terms makes this algorithm quite computationally expensive. This is the reason we have used a 10cm x 10cm grid instead of a larger aperture. While a smaller aperture increases the time efficiency of the imaging of the algorithm, the images that we obtain will have a greater mainlobe width. This results in a reduced angle resolution.

Since the distance between the transmitter and the receiver is always smaller than $2D^2/\lambda$ for all λ (where D is the size of the largest dimension of the synthetic aperture), the imaging is always performed in the near field. If we were doing the same experiment in the far field, we could write the equation (3) as (4) after taking the first summation inside and identifying the inner sum as the Fourier transform of the channel transfer function.

$$A(t,\theta,\phi) = \left| \sum_{x=1}^{X} \sum_{y=1}^{Y} C(t - t_0, x, y) \right| \qquad (4)$$

where

$$t_0 = (1/c)(x\cos\phi\cos\theta - y\sin\phi\cos\theta) \qquad (5)$$

$C(t,x,y)$ is the complex channel impulse response at the time t and position (x,y) and c is the speed of light in free space. We are not using the z-term in the position vector $\vec{R}$ because both the transmitting and receiving antennas are at the same height. Far field imaging would allow us a faster implementation by using FFT to compute the Fourier transform, and we can even use a larger aperture to improve the angle resolution.

4 RESULTS

UWB systems can resolve more multipaths than narrowband systems due to their higher bandwidth. A study of UWB multipath propagation has recently been reported [13]. We are interested in the directions from which the power is coming at a given multipath. In order to show this, we have constructed a series of power spectrum radio images corresponding to the different multipaths. Each measurement point has a multipath at a different time from another measurement point on the synthetic aperture. However, the UWB bandwidth of 2.0 GHz in our experiment gives a time resolution of around a nanosecond. This corresponds to a distance of about 30 cm in free space (after the windowing effects). The synthetic aperture we are using has dimensions of 10 cm x 10 cm with a special resolution of 1 cm. Therefore we are not able to resolve the multipath time differences between the different positions of the receiving antenna. This

means that we can either assume the same multipath times on all the receiving points, or we can just compute an average channel impulse response taken over all the measurement points and determine the multipath from this information. We have taken the latter approach, although there is not much difference between the two. Figure 2 shows the average channel multipath profile taken over all the 100 measurements.

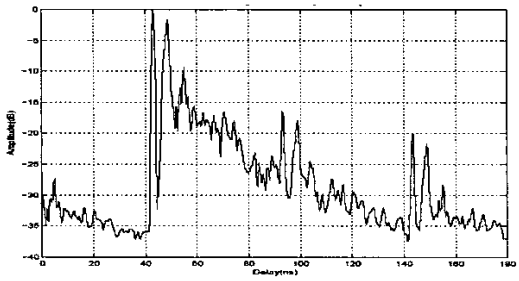

Figure 2. Magnitude of the normalized average channel impulse response (CIR).

Figure 3a-b show the power spectrum images on azimuth-elevation axes, with the intensity shown in dBs, at the first two multipaths, which occur at 42 ns and 48 ns respectively. Figure 3c shows the power spectrum image at an arbitrarily chosen time, 30 ns, for comparison. This is largely composed of background noise because the first multipath has yet to reach the receiver. A threshold of –15dB is applied to all the images, as shown in the colourbar with each figure. Note that we have shown the relative intensity images so that intensity wise comparison should not be made from one image to another.

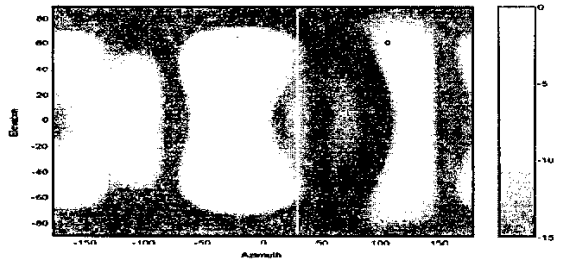

a. Image at the first multipath at 42 ns

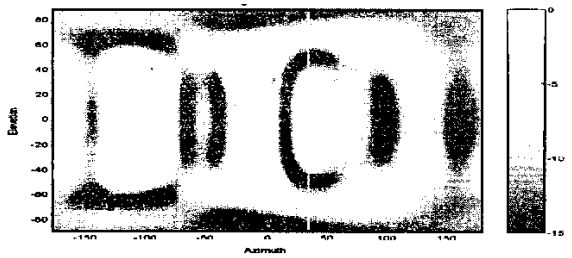

b. Image at the second multipath at 48 ns

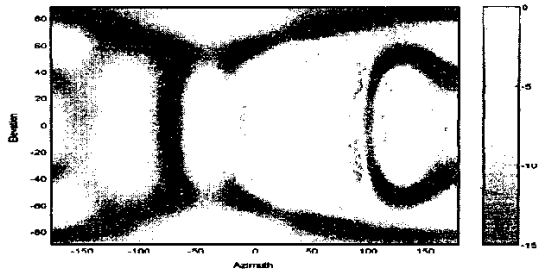

c. Image at an arbitrary time, 30 ns.

Figure 3. Power spectrum images at the first two multipaths and at an arbitrary time.

Figure 4 shows how the power spectrum varies across an arbitrarily chosen time period of 20 ns from 100 to 120 ns. The figure clearly shows the variation of the radiation pattern over time. Only 3 images are shown with time intervals of 5 ns to avoid putting many figures. We have not included the negative elevation angles in this figure to save space and improve clarity, since the negative elevation has the same information as the positive one due to the up-down ambiguity mentioned earlier.

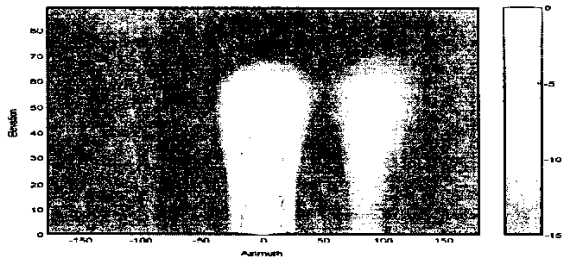

a. At 105 ns

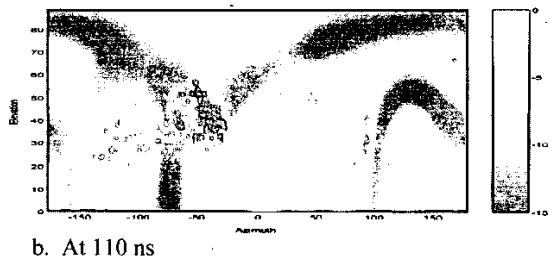

b. At 110 ns

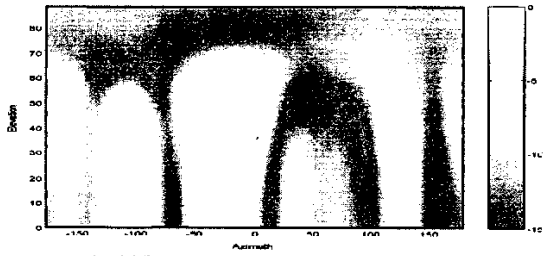

c. At 115 ns

Figure 4. Power spectrum images for an arbitrary time period.

All the images shown in figures 3 and 4 have a wide mainlobe. (Note that the sidelobes have been windowed already). This means that the angle resolution is very low. This can be improved by using a larger aperture. Since we would like to limit the size of the synthetic aperture, we can adapt the narrowband techniques of best estimator for the angle through a variety of estimation methods [10]. This constitutes part of our ongoing research in the Communications Research Group at the University of Oxford.

5 CONCLUSIONS

We have presented the indoor imaging study of UWB channels using angle of arrival calculations. We have described the imaging and signal processing methods to acquire and display the information in a visual manner. There is a lot of room for improvement in the imaging algorithm in terms of the tradeoffs between its efficiency of performance and the accuracy of angular information it provides. We believe that further research in this direction is worthwhile for efficient implementations of radio channel studies, location finding systems and short-range radars.

REFERENCES

[1] A. M. Street, J. G. O. Moss, D. J. Edwards, and M. J. Mehler, "Indoor Propagation Measurements at 5GHz," in *IEE Colloq. on Indoor Radio Propagation*, 1995.

[2] J. G. O. Moss, "Spread Spectrum Techniques for Future Communications Systems," in *Department of Engineering Science*. Oxford: University of Oxford, 1998.

[3] M. I. Skolnik, *Introduction to Radar*, Third ed: McGraw-Hill International Editions, 2001.

[4] D. D. Ferris and N. C. Currie, "Microwave and Milimeter-wave Systems for Wall Penetration," in *SPIE Conference on Target and Backgrounds*, vol. 3375. Orlando, FL, 1998, pp. 269-279.

[5] M. G. M. Hussain, "Principles of High-Resolution Radar Based on Nonsinusoidal Waves Part 1: Signal Representation of Pulse Compression," *IEEE Trans. Electromagnet. Compat.*, vol. EMC-31, pp. 359-375, 1989.

[6] M. G. M. Hussain, "Principles of High-Resolution Radar Based on Nonsinusoidal Waves Part II: Generalized Ambiguity Function," *IEEE Trans. Electromagnet. Compat.*, vol. EMC-31, pp. 369-375, 1989.

[7] M. G. M. Hussain, "Principles of High-Resolution Radar Based on Nonsinusoidal Waves Part III: Radar target Reflectivity Model.," *IEEE Trans. Electromagnet. Compat.*, vol. EMC-32, pp. 144-152, 1990.

[8] M. G. M. Hussain, "Ultra-Wideband Impulse Radar-An Overview of the Principles," *IEEE AES Systems Magazine*, pp. 9-14, 1998.

[9] J. D. Taylor, *Ultra-wideband Radar Technology*: CRC Press, 2000.

[10] S. Haykin, "Array Signal Processing," in *Prentice-Hall Signal Processing Series*, A. V. Oppenheim, Ed.: Prentice-Hall, 1985.

[11] A. M. Street, L. Lukama, and D. J. Edwards, "Use of VNAs for wideband propagation measurements," *IEE Proc. Commun.*, vol. 148, 2001.

[12] J. G. O. Moss, A. M. Street, and D. J. Edwards, "Wideband radio imaging technique for multipath environments," *IEE Electronics Letters*, vol. 33, pp. 941-942, 1997.

[13] W. Q. Malik, D. J. Edwards, and C. J. Stevens, "Experimental evaluation of Rake receiver performance in a line-of-sight ultra-wideband channel," in *Proceedings of the IEEE International Workshop on Ultra Wideband Systems joint with Conference on Ultra Wideband Systems and Technologies*. Kyoto, Japan, 18-21 May 2004.